ELASTIC RESPONSE OF CRIMPED COLLAGEN FIBRILS

A. D. FREED AND T. C. DOEHRING

ABSTRACT. A physiologic constitutive expression is presented in algorithmic format for the elastic response of wavy collagen fibrils found in soft connective tissues. The model is based on the observation that crimped fibrils have a three-dimensional structure at the μm scale that we approximate as a helical spring. The symmetry of this waveform allows the force/displacement relationship derived from Castigliano's theorem to be solved in closed form. Model predictions are in good agreement with experimental observations for mitral-valve chordæ tendineæ.

1. INTRODUCTION

Passive soft tissues are multi-constituent materials that, from a load carrying point of view, are predominantly composed of two elastic substances (elastin and collagen) immersed in a hydrated proteoglycan gel (ground substance) [1]. The elastin/gel mixture (ground substance matrix) contributes to the overall isotropic response of soft tissues. Unorganized collagen filaments with random orientations also contribute to the response of the ground substance matrix [2]. Organized collagen fibers, on the other hand, form fibrous networks that introduce anisotropic attributes into the tissue response [3].

The objective of this paper is to derive a physically based material model that is capable of describing the elastic response of soft tissues comprised of crimped collagen fibers.

1.1. Collagen Structure.

Collagen molecules are built from polypeptide chains [2]. These molecules are synthesized within cells as a tropocollagen, and then secreted into the surrounding connective tissue through cell vesicles. The tropocollagen polymer has a triple-helix geometry whose length is about 285 nm and whose diameter is 1.4 nm. A single tropocollagen self-assembles with four other tropocollagen in the extracellular matrix at quarter-stagger intervals of 67 nm (D period) to form a micro-fibril whose diameter is about 3.5 nm [4]. Glycosaminoglycans (GAG's) serve as the cross-linking agent in this assembly process, with chemical attachments primarily located at the D-period banding sites. Micro-fibrils are gathered together via lateral and end-to-end aggregations to form sub-fibrils with a 10–20 nm diameter, which themselves aggregate to form fibrils with a 50–500 nm diameter [5]. The outcome is a slender, flexible fibril with fractal geometry.

Date: 14th May 2004.

Funding for ADF came from the US DoD (DAMD17-01-1-0673) to the Cleveland Clinic, Dr. Ivan Vesely (PI), conducted under Space Act Agreement SAA3-516. Funding for TCD came from the US NIH (NHLBI HL 72598).

ASME PAPER NO. IMECE 2004-61578

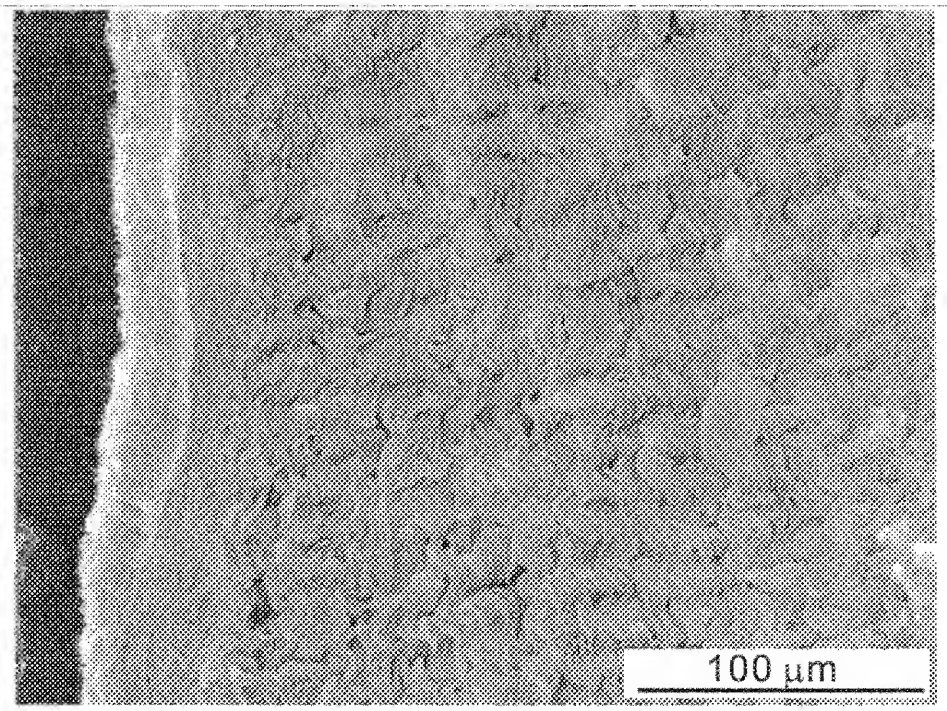

FIGURE 1. SEM photograph of a cross-sectional cut of a chordæ tendeneæ taken from a porcine mitral valve showing a 3D undulating fiber structure. (Reproduced with permission from J. Liao [6].)

Fibrils are the fibrous entities observed in photographic images taken by scanning electron microscopes, like the image presented in Fig. 1.

Fibrils are assembled by the human body in a variety of ways to meet the varying needs of its soft tissues. Because the aspect ratio of a fibril is huge (2000 to 2500 [7]), it readily buckles under the internal restoring forces of the elastin matrix whenever a fibrous tissue is free from external load [8]. This rumpled configuration is known as crimp (see Fig. 1). Crimp occurs at the level of a fascicle—an aggregate of fibrils—which is the sixth tier in the collagen hierarchy [5]. Collagen fibers are assemblages of fibrils or fasciclæ, depending on the tissue; for example, chordæ tendineæ are 'yarns' of fibrils (i.e., a fascicle), while tendons are 'ropes' of fascicles. The wavy structure of crimp has a periodicity of between 10 and 100 μm, depending on the tissue. Tissues with shorter wavelengths tend to have greater extensibility's, as there seems to be less variability in crimp amplitude between tissues [6].

The elastic modulus of a collagen molecule is about 3 GPa. A collagen fibril has an elastic modulus in the mid 100's of MPa [9]. Both have linear stress/strain responses. The existence of crimp in aggregates of fibrils is the primary cause of the characteristic nonlinear response which is so prevalent in soft-tissue data. The nonlinear effect that crimp has on mechanical response has been known for nearly a century [10]. Crimped collagen tissues typically have an elastic modulus in the upper 10's to lower 100's of MPa when measured in the linear region. The elastic modulus therefore appears to decrease as lower-level assemblages aggregate into higher-level architectures in the collagen-fiber hierarchy [9]; however, there are conflicting data in this regard [11].

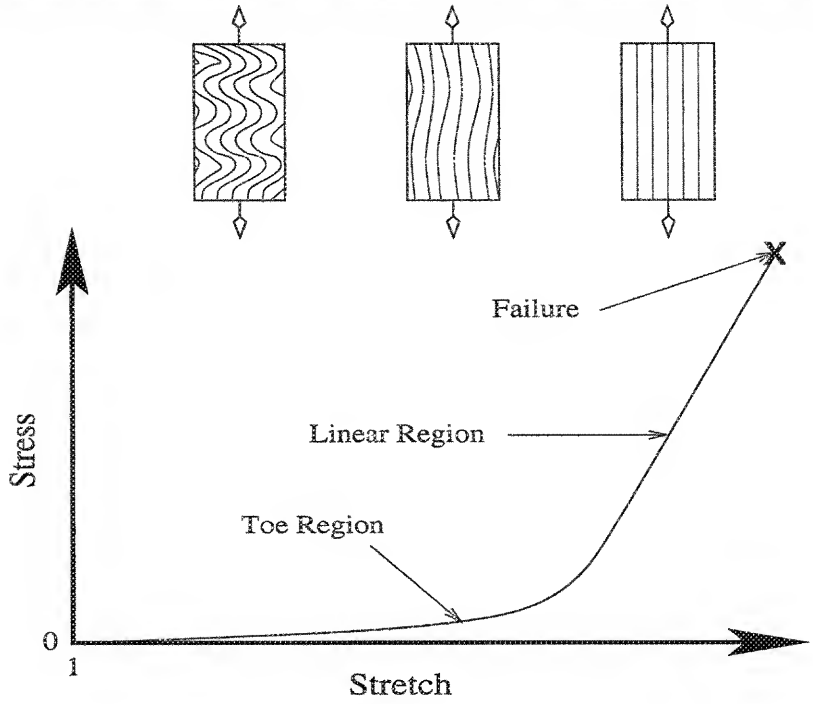

FIGURE 2. A schematic of the stress/stretch response of collagenous tissues, and how their wavy structures vary with deformation.

1.2. **Collagen Models.** The response of collagen dominated tissues to external loads can be divided into two regions, as shown in Fig. 2. In the first region, called the toe or toe/heel region, collagen undulates carrying load as if it were an uncoiling spring. No stretching at the micro-fibril level is observed—the D-spacing remains constant throughout the toe region [12].

As the deformation leaves the toe region, passing the heel in the stress/stretch curve, the response enters a nearly linear domain of substantial stiffness. Here the collagen fibrils have been stretched from their former wavy shape into a straightened configuration. Stretch arises from several mechanisms in the linear region. The D-spacing at the micro-fibril level has been observed to extend from 67 nm up to 69 nm, but this only contributes about 40% to the overall stretch [12]. Another possible mechanism for stretch is the deformation of mechanical linkages binding the various tiers in the collagen hierarchy—a folding over and extension of the GAG cross-links [6]. The extent that this combined shear-lag/fluid-transport effect contributes to the overall elastic stiffness is unknown. Our physical model also suggests that another contribution to this mechanism of deformation may actually belong to the heel region: the final stretching of crimp into its taut state (cf. Fig. 7).

Fiber tearing generally occurs at the end of stretching in the linear region. Fibrils tear; they do not deform plastically, although plasticity concepts have been applied to them [2]. Figure 2 represents the response of a single crimped fibril. A fiber is a collection of fibrils, wherein the failure of individual fibrils occur at different states producing a collective stress/strain response (beyond the toe region) whose eventual failure is more gradual and graceful than that of an individual fibril.

Material models for collagen generally belong to one of two classes: phenomenological or structural. Both micro and macro variants belonging to these material classes have been constructed.

Phenomenological models have material parameters with no direct morphological basis. The exponential function is most commonly employed in such descriptions of collagen [13]. Power-law functions have also been used with good success in the modeling of collagen [14].

Structural models have physiologic parameters. There are predominantly two types of structural crimp models that have been reported on in the literature. Both consider 2D waveforms for describing crimp. They are outgrowths from two distinct camps of thought: one being that crimp has a fairly smooth planar waveform like a sinusoid, and the other being that crimp has a more jagged planar waveform like a sawtooth. Both collectives base their hypothesis upon microscopic evidence.

Comninou and Yannas [15] and Lanir [1] derived constitutive formulæ for collagen fibers from a sinusoidal waveform for crimp, as advocated by Dale et al. [16]. Both models were shown to correlate experimental data reasonably well. Lanir's model adds a fiber/matrix (i.e., collagen/elastin) interaction effect.

Zig-zag models based on kinematic linkages with rigid hinges and flexible links [17], with flexible hinges and rigid links [18], and with flexible hinges and flexible links [19] constitute a second class of assumed collagen fiber waveforms. They correlate data with varying degrees of realism.

In contrast, our collagen model assumes a smooth 3D waveform for describing crimp; specifically, we employ a cylindrical helix. Evans and Barbenel [20] and Yahia and Drouin [21] have both reported that planar and helical crimp patterns exist. The waveform shape depends on both tissue and location. Lerch [22] was the first to describe the geometric features of crimp, and this he did using the geometry of a cylindrical helix for representing crimp waveform. Beskos and Jenkins [23] were the first, and apparently the only ones to derive a constitutive expression for crimped collagen based on a cylindrical helix for the waveform. However, their model predicts an infinite stiffness at full extension due to an assumption of fiber in-extensibility, which is not realistic.

In measurements of crimp angle vs. strain, Dale et al. [16] observed actual tissue behavior to be bounded between models of an extending sine wave (from below) and an extending cylindrical helix (from above). In this paper we derive a physiologically based constitutive expression at the μm scale for the helical bound.

Lanir [24] proposed assembling an aggregate of micro-constitutive fibril models oriented in various directions that are averaged via a probability distribution function, thereby resulting in a homogenized macro-constitutive equation appropriate for tissue modeling. Expounding upon this idea, we [25] have derived a constitutive expression for soft tissues that accounts for fiber splay in an efficient manner, thereby making it suitable for finite-element implementation. This continuum model requires $\sigma(\lambda)$ and $\mathrm{d}\sigma(\lambda)/\mathrm{d}\lambda$ as material inputs, where σ is the fiber stress and λ is the fiber stretch. The paper you are reading resulted from our need to know these material functions, and our desire to derive them from a physiologic representation of collagen crimp.

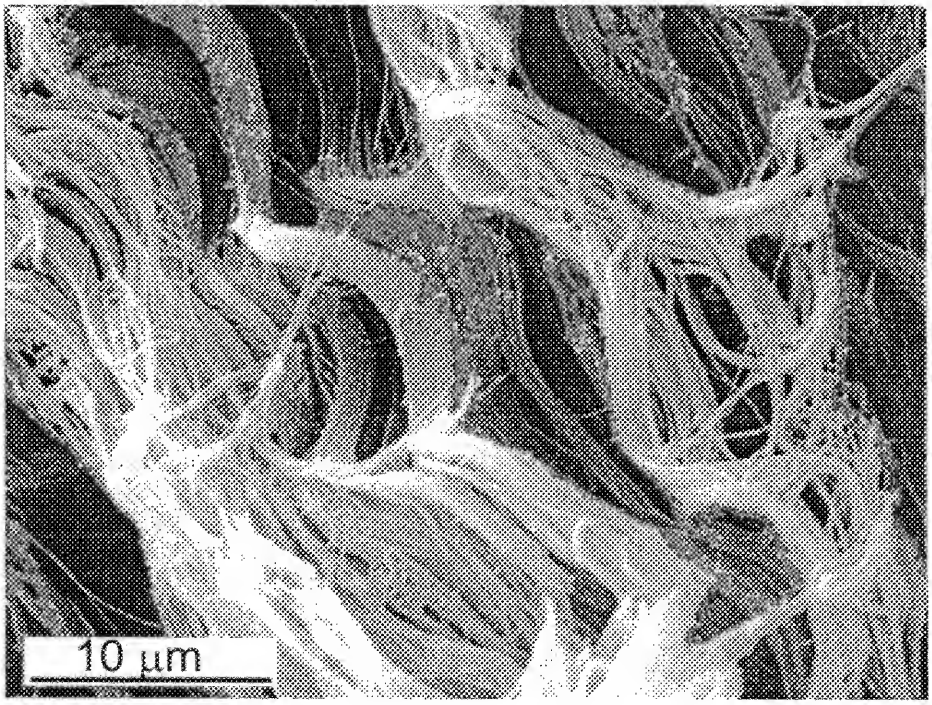

FIGURE 3. SEM photograph showing the helical nature of crimped collagen fibrils in chordæ tendeneæ taken from a porcine mitral valve. (Reproduced with permission from J. Liao [6].)

2. GEOMETRIC MODEL FOR COLLAGEN FIBRILS IN A FASCICLE

Figure 3 is a close-up of Fig. 1, where one observes that collagen fibrils have a 3D helical shape in a fascicle free from external traction. Three different protocols were followed for SEM specimen preparation, all resulting in images of crimped collagen fibrils that undulate in 3-space [6].

By exploiting the geometry of a cylindrical helix, we have been able to derive a physiologically based material model that can represent the nonlinear stress/strain response of soft collagenous tissues. An advantage of adopting a cylindrical helix for representing the waveform of crimp is that the symmetry of its geometry mitigates the need to integrate along the helical axis, thereby resulting in a closed-form algebraic constitutive expression.

2.1. Geometry of a Cylindrical Helix.

Consider a fibril in a reference frame that is free from external traction, and assume that this fibril takes on the shape of a cylindrical helix. Let the height (or wavelength) of this helix be denoted by H, which has a typical value ranging between 10 and 100 μm, and let its radius (or amplitude) be given by R, which has a typical value ranging between 1 and 10 μm [4]. Consequently, the chord length L of one helical revolution is determined to be $L = (4\pi^2 R^2 + H^2)^{1/2}$—a parameter that we shall assume remains fixed throughout deformation in the toe region. Furthermore, let the radius of this fibril be denoted by r—another parameter that we assume remains fixed, but whose value can vary between 50 and 500 nm depending on age, tissue, and location within the tissue [4].

When modeling a particular tissue, the three physiologic parameters H, R, and r represent statistical averages taken over the volume.

A cylindrical-polar coordinate system was employed by Ancker and Goodier [26] in their classic study of helical springs, and by Beskos and Jenkins [23] in the development of their collagen model. We, on the other hand, adopt the coordinate system of differential geometry, where the geometry of any curve in 3-space can be described by an orthogonal triad of unit base vectors, which for a cylindrical helix is given by [27, pg. 27]

$$\begin{aligned} \hat{\mathbf{t}} &= \omega\big(-R\sin\omega s,\ R\cos\omega s,\ H\big), \\ \hat{\mathbf{n}} &= \big(-\cos\omega s,\ -\sin\omega s,\ 0\big), \\ \hat{\mathbf{b}} &= \omega\big(H\sin\omega s,\ -H\cos\omega s,\ R\big), \end{aligned} \tag{1}$$

wherein $\hat{\mathbf{t}}$ is the tangent vector, $\hat{\mathbf{n}}$ is the normal vector, and $\hat{\mathbf{b}}$ is the binormal vector. Parameter s designates a location along the curve, while $\omega = (R^2+H^2)^{-1/2}$. Curvature κ and torsion τ (properties of curves in space) are equal in a helix, with $1/\kappa$ being the radius of curvature. For a cylindrical helix, $\kappa = R/(R^2+H^2)$ with $R > 0$.

2.2. **Extension of a Cylindrical Helix.** Figure 4 presents a schematic of how a helical collagen fibril is considered to carry load. A force $\mathbf{P} = (0, 0, P)$ is assumed to act along the centerline of the helix in the 3-direction, which is consistent with spring theory [26]. This load translates out to the helix mean radius R, thereby producing normal $\mathbf{F}$ and shearing $\mathbf{V}$ forces that act on the face of the helix in directions $\hat{\mathbf{t}}$ and $\hat{\mathbf{b}}$, respectively, such that

$$\begin{aligned} \mathbf{F} &= (\mathbf{P}\cdot\hat{\mathbf{t}})\hat{\mathbf{t}} = F\,\hat{\mathbf{t}}, \qquad & F &= PH/\sqrt{R^2+H^2}, \\ \mathbf{V} &= (\mathbf{P}\cdot\hat{\mathbf{b}})\hat{\mathbf{b}} = V\,\hat{\mathbf{b}}, \qquad & V &= PR/\sqrt{R^2+H^2}, \end{aligned} \tag{2}$$

where $\mathbf{P}\cdot\hat{\mathbf{n}} = 0$. The act of moving $\mathbf{P}$ to the helix backbone also produces a bending moment $\mathbf{M}$ and a torque $\mathbf{T}$ that are quantified by

$$\begin{aligned} \mathbf{M} &= R\,\hat{\mathbf{n}}\times F\,\hat{\mathbf{t}} = -RF\,\hat{\mathbf{b}} = -M\,\hat{\mathbf{b}}, \qquad & M &= PRH/\sqrt{R^2+H^2}, \\ \mathbf{T} &= R\,\hat{\mathbf{n}}\times V\,\hat{\mathbf{b}} = RV\,\hat{\mathbf{t}} = T\,\hat{\mathbf{t}}, \qquad & T &= PR^2/\sqrt{R^2+H^2}. \end{aligned} \tag{3}$$

Scalars P, F, V, M, and T are the magnitudes of vectors $\mathbf{P}$, $\mathbf{F}$, $\mathbf{V}$, $\mathbf{M}$, and $\mathbf{T}$, respectively.

Consider first the case of a straight filament whose strain energy is $U = \frac{1}{2}\int \sigma\epsilon\,\mathrm{d}V$, where σ is stress, ϵ is strain, and V is volume. The elastic strain energy of such a filament is $U_F = F^2L/2AE_f$, where F is the applied force, L is the length, $A = \pi r^2$ is the cross-sectional area, and E_f is the elastic modulus of the filament. An application of Castigliano's theorem [28, pp. 133–136] leads to the following force/displacement relation

$$\Delta L = \frac{\partial U_F}{\partial F} \quad \therefore \quad F = K_f\frac{\Delta L}{L} \quad \exists \quad K_f = AE_f,$$

where ΔL is the change in length, and K_f is the filament stiffness.

For a helix, one must add to the strain energy for stretch U_F, the strain energies for shear $U_V = 20V^2L/9AG_f$, bending $U_M = M^2L/2IE_f$, and torsion $U_T = T^2L/2JG_f$, where $I = \frac{1}{4}\pi r^4$ and $J = \frac{1}{2}\pi r^4$ are the moment of inertia and polar-moment of inertia, respectively, with G_f denoting the shear modulus of the filament, which we take to

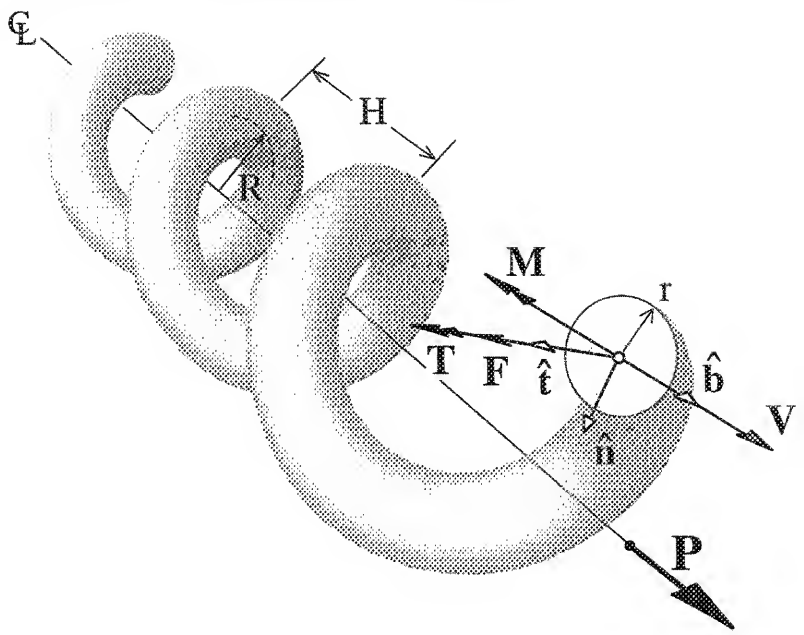

FIGURE 4. Diagram of how force **P** acting along the centerline of a helix is transferred to forces **F** and **V** and moments **M** and **T** that act along the backbone of the helix.

be $G_f = E_f/3$. Another application of Castigliano's theorem, this time using Eqs. (2 & 3), leads to

$$\Delta H = \frac{\partial(U_F + U_V + U_M + U_T)}{\partial P} \tag{4a}$$

and therefore

$$P = K\frac{\Delta H}{H} \quad \exists \quad K = K_f \frac{R^2 + H^2}{LH\big(1 + 4R^2/r^2 + 6(20/9 + R^2/r^2)R^2/H^2\big)}, \tag{4b}$$

with K being the elastic spring stiffness of a helix. The first term in the parentheses of the denominator arises from stretching, the second term from bending, the third term from shearing, and the forth term from twisting. All four energies are needed to obtain realistic behavior from the ensuing constitutive formula. It is the symmetry of a cylindrical helix along its length that leads to an algebraic equation for stiffness (instead of an integral equation), which adds great utility to the resulting model.

Unlike classical spring theory, where the ratio of radii ($r/R < 0.25$) and the angle of pitch ($\phi = \tan^{-1} H/4R < 15°$) of a helix are constrained so that the spring stiffness remains approximately linear with deformation [26], the physics of crimped collagen requires the helix to stretch straight. A plot of changes in the amplitude R and angle of pitch ϕ over the toe region, whose responses are almost identical, is presented in Fig. 5.

Linear beam theory was used in the derivation of Eq. (4b) as an approximation. We also employed the Winkler-Bach flexure formula from curved beam theory [29,

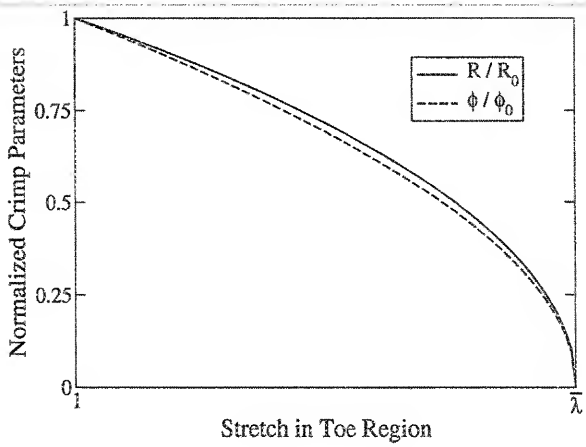

FIGURE 5. Plots of the amplitude R and angle of pitch ϕ of crimp (normalized by their initial values R_0 and ϕ_0) vs. stretch λ over the toe region.

pg. 142] and found the additional effects due to curvature to be negligible for helical geometries representative of crimp.

2.3. **Constitutive Formulation.** Our helical model for collagen appears to have three, independent, geometric parameters (viz., H_0, R_0, and r_0) but, in fact, there are only two. This is demonstrated in Fig. 6, where two different curves for H_0/r_0 are plotted against a normalized stiffness $E/\bar{E}$, wherein E is the elastic modulus of the linear region, and $\bar{E}$ is that secant modulus belonging to the point of transition between the toe and linear regions. In one curve, H_0 is held constant and r_0 is varied, while in the other curve, r_0 is held constant and H_0 is varied. The two curves are identical. Consequently, one is free to choose the dimensionless ratios H_0/r_0 and R_0/r_0 as the independent variables.

The derivation of our constitutive equation for collagen, which is outlined in Alg. 1, was founded upon the following set of assumptions:

(1) The waveform used to represent crimp is that of a cylindrical helix which extends into a straightened configuration in the linear region of deformation.
(2) The only load carried by a crimped fibril is an axial force acting along the centerline of the helix, which is consistent with spring theory, torsion springs withstanding.
(3) Micro-structurally, the chord of a helix deforms elastically, in accordance with linear (infinitesimal deformation) theory. Macro-structurally, the helical fiber deforms in accordance with finite-deformation theory.
(4) No interactions are considered between neighboring helices (e.g., there is no fiber recruitment [30] or out-of-phase wave pattern [31]), or between a fibril and the ground substance matrix [1].
(5) The molecular dimensions along the backbone of a helix remain fixed over a deformation history when loaded in the toe region.

Whenever the mean radius R of a helix is positive, the deformation is said to be in the toe region. Whenever this radius becomes zero, the deformation is said to be in

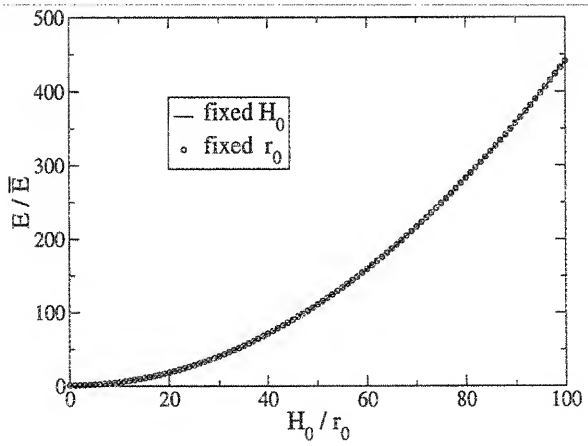

FIGURE 6. Plots of crimp wavelength H_0 normalized by fibril radius r_0 (where in one curve H_0 varies, and in the other curve r_0 varies) vs. the elastic modulus E normalized by the secant modulus $\bar{E}$ evaluated at the end of the toe region.

Algorithm 1.
Given H_0/r_0, R_0/r_0, E, *and* λ_u, *where* H_0 *is the initial wavelength of crimp,* R_0 *is the initial amplitude of crimp,* r_0 *is the initial fibril radius,* E *is the elastic modulus of the fiber in the linear region, and* λ_u *is its ultimate stretch, then:*

Set $r_0 = 1$ *so that* $H_0 \equiv H_0/r_0$ & $R_0 \equiv R_0/r_0$.

Compute constant parameters:

$L_0 = \left((2\pi R_0)^2 + H_0^2\right)^{1/2}$,

$\bar{\lambda} = L_0/H_0 < \lambda_u$,

$\bar{E} = E/\{(H_0/L_0)^2 + [H_0(L_0 - H_0)/L_0^2][1 + 37/6\pi^2 + 2(L_0/\pi r_0)^2]\}$.

If $\lambda \leq \bar{\lambda}$ *Then*

(Yes, compressive stretches, i.e., $0 < \lambda < 1$, are allowed.)

$H = \lambda H_0$,

$R = (L_0^2 - H^2)^{1/2}/2\pi$,

$\xi = (R^2 + H^2)/\{L_0 H[1 + 4R^2/r_0^2 + 6(20/9 + R^2/r_0^2)R^2/H^2]\}$,

$\sigma = \bar{E}\xi(\lambda - 1)/\lambda$

Else If $\bar{\lambda} \leq \lambda \leq \lambda_u$ *Then*

$\sigma = \bar{E}(\bar{\lambda} - 1)/\bar{\lambda} + E(\lambda - \bar{\lambda})$

Else (Fibril Failure)

$\sigma = 0$.

Return σ.

the linear region. The first four assumptions stated above were used in the derivation of Eq. (4). The fifth assumption allows Eq. (4) to be uncoupled so that stiffness only depends on geometric parameters. Coupling would arise if the chord length L were allowed to extend elastically whenever $R > 0$. Figure 7 demonstrates the wide range of material behavior that Alg. 1 can reproduce.

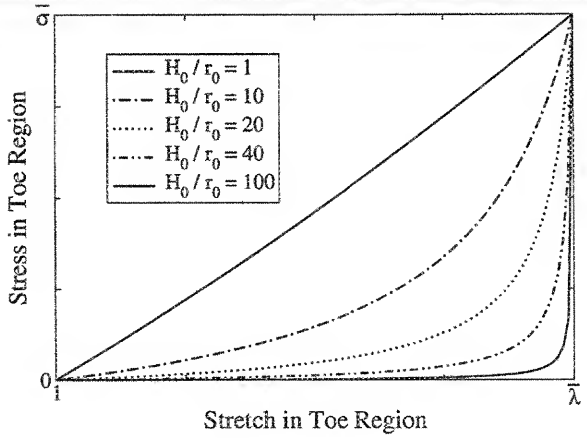

FIGURE 7. Various shapes for stress/stretch curves in the toe region, where $\bar{\lambda}$ and $\bar{\sigma} = \bar{E}(\bar{\lambda}-1)/\bar{\lambda}$ are the stretch and stress values belonging to the point of transition between the toe and linear regions. The linear region is not plotted.

Algorithm 1 applies to a fibril. It requires four material constants to be specified: H_0/r_0, R_0/r_0, E, and λ_u. Given an axial stretch λ for a fiber, the algorithm returns the stress σ carried by that fiber. In this algorithm, $\bar{\lambda}$ and $\bar{E}$ represent the stretch and secant modulus, respectively, at the point of transition between the toe and linear regions. Parameter ξ was extracted from Eq. (4b). Of the four specified material parameters, the stretch at failure λ_u and the elastic modulus E (over the linear region) can both be obtained directly from an experimental stress/strain curve. Acquiring the remaining two parameters, H_0/r_0 and R_0/r_0, is a more arduous task that is greatly aided by optimization techniques.

Unlike other collagen fiber models, our model permits compressive states—a helical spring can compress. These states are very soft.

Like the collagen model of Hurschler et al. [32], our model accounts for failure. Fibril failure is represented in a boolean manner. Fiber failure, to be correctly modeled, would need to be an integral sum over all fibrils in a fiber, which is beyond the scope of this paper.

3. EXAMPLE

Many passive soft tissues act as tethers, transmitting loads from one attachment point to another in a one-dimensional manner; for example: tendons, ligaments, and the chordæ tendineæ of heart valves. Under normal loading conditions, the forces carried by individual fibrils in these materials act along the centerlines of their helices. Most experiments done on soft tissues are also one-dimensional, with the axis of loading and the dominant fiber axis being coincident. Algorithm 1 applies to these test conditions.

The ability of our helical model to fit experimental data is demonstrated in Fig. 8. The data presented therein are from five chordæ tendineæ taken from porcine mitral valves. The experiments were done in a servo-hydraulic testing system using a protocol that is described in Ref. [33]. The cross-sectional areas and gage lengths

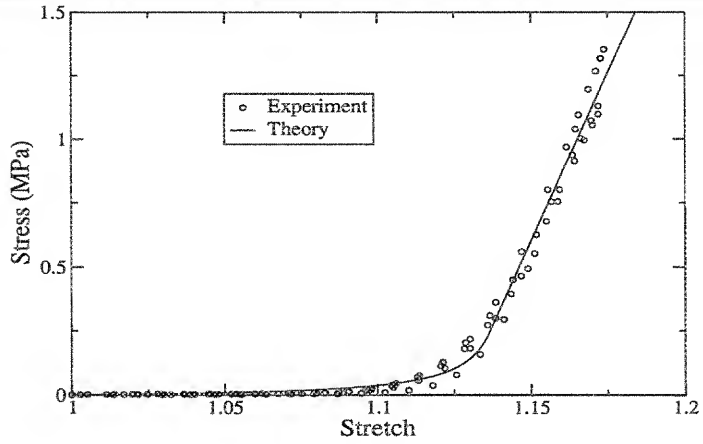

FIGURE 8. A fit of the helix model to data taken from five, porcine, mitral-value, chordæ-tendineæ specimens.

of these five specimens were measured in their unloaded state. They were gripped using sinusoidal clamps, and immersed in a temperature controlled (37C) saline bath. An uniaxial ramp displacement (10 mm/s) was applied, and the resulting loads were recorded. Stretch was computed from the grip-to-grip displacement, while stress was computed from the measured load divided by the original cross-sectional area.

Helical model parameters were estimated using the direct-fit method described in Ref. [14]. The direct-fit method uses a grid-based global optimization approach to fit the model to the actual point-wise stress/stretch data. A single model fit was done using the data from all five specimens grouped together. Gage lengths were originally computed using an established protocol [34]. Because of the difficulty of assigning an accurate gage length to soft-tissue experiments, these original lengths were then manually adjusted (by $< 0.5\%$) so that the linear portions of the stress/stretch curves came into good alignment. The resulting optimal model parameters were: $H_0/r_o = 21.0$, $R_0/r_0 = 1.80$, and $E = 26.6$ MPa; with a residual sum-of-squares error of 0.0072.

4. DISCUSSION

A physiological model for collagen tensile behavior can be useful for elucidating structure-function relationships, and for assessing the mechanical behavior of tissues. The work presented in this paper provides a theoretical framework for representing collagen crimp based on the geometry of a cylindrical helix. We chose this helix geometry because recent morphological evidence indicates a helical structure for crimped collagen [6]. Indeed, helix-type structures are common in biological materials, e.g., DNA. Hence, the helix model developed herein may be useful in studies for a variety of biological materials.

The low residual error obtained indicates that our helical model fits the data well, particularly in the toe region. The model fit is not as good in the heel region, however, having a stronger curvature and a more abrupt transition between the toe and linear regions than is otherwise apparent in the data. Additionally, in the linear region, the data tend to retain a small amount of curvature that is not represented by the model.

These behaviors could be accounted for by including fiber recruitment, which would tend to soften the curvature as fibers are gradually stretched. Including recruitment into the model is a subject of current study.

We were encouraged to find that the resulting optimal parameters for our relatively simple helical model corresponded well to the measured wavelengths and amplitudes of crimp observed in optical and SEM images of the chordæ. This further supports the hypothesis that a cylindrical helix representation may be representative of the actual tissue micro-structure. Further applications to tensile testing of specimens with different crimp patterns (e.g., pericardium, rat-tail tendon, etc.) are needed to investigate possible relationships between model parameters and tissue micro-structure.

Results from this chordæ example suggest that the helical model can be used to approximate the elastic response of crimped collagen in uniaxial tension. This helical model has the potential to represent a wide variety of materials that possess a helical-type structure, and has been incorporated into our ongoing efforts to model various facets of soft-tissue mechanics that includes physiologic fiber splay, recruitment, and viscoelastic behaviors.

Acknowledgment

The authors takes this opportunity to thank Drs. Daniel Einstein, Jun Liao, and Ivan Vesely for many delightful discussions on this and related topics.

References

[1] Lanir, Y., 1978, "Structure-Strength Relations in Mammalian Tendon," Biophys. J., **24**, pp. 541–554.

[2] Viidik, A., 1973, "Functional Properties of Collagenous Tissues," Int. Rev. Connect. Tiss., **6**, pp. 127–215.

[3] Humphrey, J. D., 2002, "Continuum Biomechanics of Soft Biological Tissues," Proc. Roy. Soc. London, **A–459**, pp. 3–46.

[4] Nimni, M. E. and Harkness, R. D., 1988, "Molecular Structure and Functions of Collagen," in: *Collagen*, Nimni, M. E., ed., vol. I, Biochemistry, chap. 1, CRC Press, Boca Raton, pp. 1–77.

[5] Kastelic, J., Galeski, A., and Baer, E., 1978, "The Multicomposite Structure of Tendon," Connect. Tissue Res., **6**, pp. 11–23.

[6] Liao, J., 2003, "Mechanical and Structural Properties of Mitral Valve Chordæ Tendineæ," Ph.D. thesis, Cleveland State University, Cleveland, Ohio.

[7] Trotter, J. A., Thurmond, F. A., and ???, 1994, "Molecular Structure and Functional Morphology of Echinoderm Collagen Fibrils," Cell Tissue Res., **275**, pp. 451–458.

[8] Weiss, J. A. and Gardiner, J. C., 2001, "Computational Modeling of Ligament Mechanics," Crit. Rev. Biomed. Eng., **29**, pp. 303–371.

[9] Sasaki, N. and Odajima, S., 1996, "Elongation Mechanism of Collagen Fibrils and Force-Strain Relations of Tendon at Each Level of Structural Hierarchy," J. Biomech., **29**, pp. 1131–1136.

[10] Nauck, E. T., 1931, "Die Wellung der Sehnenfasern, ihre Ursache und ihre funktionelle Bedeutung," Gegenbaurs Morph. Jahrb., **68**, pp. 79–96.

[11] Miyazaki, H. and Hayashi, K., 1999, "Tensile Tests of Collagen Fibers Obtained from the Rabbit Patellar Tendon," Biomed. Microdevices, **2**, pp. 151–157.

[12] Fratzl, P., Misof, K., Zizak, I., Rapp, G., Amenitsch, H., and Bernstorff, S., 1997, "Fibrillar Structure and Mechanical Properties of Collagen," J. Struct. Biol., **122**, pp. 119–122.

[13] Fung, Y.-C., 1967, "Elasticity of Soft Tissues in Simple Elongation," Am. J. Physiol., **213**, pp. 1532–1544.

[14] Doehring, T. C., Carew, E. O., and Vesely, I., 2004, "The Effect of Strain Rate on the Viscoelastic Response of Aortic Valve Tissue: A direct-fit approach," Ann. Biomed. Eng., **32**, pp. 223–232.

[15] Comninou, M. and Yannas, I. V., 1976, "Dependence of Stress-Strain Nonlinearity of Connective Tissues on the Geometry of Collagen Fibers," J. Biomech., **9**, pp. 427–433.

[16] Dale, W. C., Baer, E., Keller, A., and Kohn, R. R., 1972, "On the Ultrastructure of Mammalian Tendon," Experientia, **28**, pp. 1293–1295.

[17] Diamant, J., Keller, A., Baer, E., Litt, M., and Arridge, R. G. C., 1972, "Collagen; ultrastructure and its relation to mechanical properties as a function of aging," Proc. Royal Soc. London, **B–180**, pp. 293–315.

[18] Kastelic, J., Palley, I., and Baer, E., 1980, "A Structural Mechanical Model for Tendon Crimping," J. Biomech., **13**, pp. 887–893.

[19] Stouffer, D. C., Butler, D. L., and Hosny, D., 1985, "The Relationship Between Crimp Pattern and Mechanical Response of Human Patellar Tendon-Bone Units," ASME J. Biomech. Eng., **107**, pp. 158–165.

[20] Evans, J. H. and Barbenel, J. C., 1975, "Structure and Mechanical Properties of Tendon related to Function," Equine Vet. J., **7**, pp. 1–8.

[21] Yahia, L. and Drouin, G., 1989, "Microscopical Investigation of Canine Anterior Cruciate Ligament and Patellar Tendon: Collagen fascicle morphology and architecture," J. Orthop. Res., **7**, pp. 243–251.

[22] Lerch, H., 1950, "Über den Aufbau des Schnengewebes," Gegenbaurs Morph. Jahrb., **90**, pp. 192–205.

[23] Beskos, D. E. and Jenkins, J. T., 1975, "A Mechanical Model for Mammalian Tendon," ASME J. Appl. Mech., **42**, pp. 755–758.

[24] Lanir, Y., 1983, "Constitutive Equations for Fibrous Connective Tissues," J. Biomech., **16**, pp. 1–12.

[25] Freed, A. D., Einstein, D. R., and Vesely, I., 2004, "Invariant Theory for Dispersed Transverse Isotropy: An efficient means for modeling fiber splay," ASME IMECE 2004/61236.
[26] Ancker, Jr., C. J. and Goodier, J. N., 1958, "Theory of Pitch and Curvature Corrections for the Helical Springs—I (Tension)," ASME J. Appl. Mech., **25**, pp. 471–483.
[27] Millman, R. S. and Parker, G. D., 1977, *Elements of Differential Geometry*, Prentice-Hall, Englewood Cliffs.
[28] Langhaar, H. L., 1962, *Energy Methods in Applied Mechanics*, John Wiley & Sons, New York.
[29] Seely, F. B. and Smith, J. O., 1952, *Advanced Mechanics of Materials*, 2nd ed., John Wiley & Sons, New York.
[30] Belkoff, S. M. and Haut, R. C., 1991, "A Structural Model Used to Evaluate the Changing Microstructure of Maturing Rat Skin," J. Biomech., **24**, pp. 711–720.
[31] Rowe, R. W. D., 1985, "The Structure of Rat Tail Tendon Fascicles," Connect. Tissue Res., **14**, pp. 21–30.
[32] Hurschler, C., Loitz-Ramage, B., and Vanderby, Jr., R., 1997, "A Structurally Based Stress-Stretch Relationship for Tendon and Ligament," ASME J. Biomech. Eng., **119**, pp. 392–399.
[33] Carew, E. O., Doehring, T. C., Barber, J. E., Freed, A. D., and Vesely, I., 2003, "Fractional-Order Viscoelasticity Applied to Heart Valve Tissues," in: *Proceedings of the 2003 Summer Bioengineering Conference*, Soslowsky, L. J., Skalak, T. C., Wayne, J. S., and Livesay, G. A., eds., ASME, Key Biscayne, FL, pp. 721–722.
[34] Doehring, T. C. and Vesely, I., in review, "Influence of Gage Length Errors on Quasilinear Viscoelastic Parameter Estimates," .

Alan D. Freed, Ph.D., ASME Fellow, Senior Research Engineer, Polymers Branch, Materials Division, MS 49-3, NASA's John H. Glenn Research Center at Lewis Field, 21000 Brookpark Road, Cleveland, OH 44135, USA, And: Adjunct Staff, Department of Biomedical Engineering, ND-20, The Cleveland Clinic Foundation, 9500 Euclid Avenue, Cleveland, OH 44195, USA
E-mail address: Alan.D.Freed@nasa.gov

Todd C. Doehring, Ph.D., Research Associate, Department of Biomedical Engineering, ND-20, Lerner Research Institute, The Cleveland Clinic Foundation, 9500 Euclid Avenue, Cleveland, OH 44195, USA
E-mail address: tcdoe@bme.ri.ccf.org